C. Y. Poon

R. S. Sayles

Department of Mechanical Engineering,
Imperial College, Exhibition Road,
London SW7 2AZ, U.K.

Contact Analysis of a Smooth Ball on an Anisotropic Rough Surface

The effects of surface roughness and waviness upon the real contact areas, gaps between contact spots, and asperity contact pressures were studied. The distribution of real areas, gaps, and contact pressures are presented for different surface roughness, σ and correlation lengths, β^*. The load-area relationship is compared to Bush's model of strongly anisotropic rough surface contact using a stochastic approach.

1 Introduction

The tribological behavior of a surface can often be related to the surface roughness. If the roughness is high, the area of intimate surface contact is usually much less than the apparent contact area and the contact stress will be inevitably high. The mode of contact with most metals will probably be plastic. On the other extreme, if the roughness is very low, the area of contact, as will be shown later, can be relatively large and approach a value equal to the nominal are such that no gap exists between contact spots.

For rough surface contacts, there is a need to know how the contact area, gaps, and contact stresses are distributed: does the contact consist of one relatively large spot, or a large number of evenly distributed smaller spots of equal size, or (more likely) a randomly distributed number of spots of widely different sizes? As the load increases, is the increase in real area due to an increase in their number or their sizes?

In the past, stochastic techniques have been used to study rough surface contact problems, such as the proportionality of the load-area relationship (Greenwood and Williamson, 1966; Bush et al., 1975), the distribution of contact areas and their size (Greenwood 1967; Sayles and Thomas 1978; Nayak, 1971). The stochastic approaches usually assume that the discrete contact "spots" deform without interacting with each other and that the contacts tend to occur on the asperity peaks only. For nominally flat surfaces under light loads the individual contact spots may well be remote enough for these assumptions to be valid; however, for concentrated contacts, such as the contact of a sphere on a rough surface, it is not usually the case.

As the roughness of a surface decreases, the contacts can be expected to occur on valleys as well as on peaks due to elastic conformity of the longer wavelength features. The development of numerical techniques for elastic rough surface (Webster and Sayles, 1986) contact has enabled us to consider the interaction of deformation from all the contact points. Therefore, in this paper, the influence of surface roughness on the distribution of real area, contact spot, gaps and contact stresses are studied using the numerical rough surfaces contact model described by Poon and Sayles (1993).

Contributed by the Tribology Division for publication in the JOURNAL OF TRIBOLOGY. Manuscript received by the Tribology Division January 14, 1993; revised manuscript received May 10, 1993. Associate Technical Editor: C. Cusano.

2 Rough Surface Contract Analysis

A set of 11 abraded surfaces were prepared using silicon carbide abrasive paper of different grit size to produce different spatial structures. The surface parameters are characterized (White House and Archard, 1970) by the rms roughness σ of the height distribution, and the correlation length β^* which describes the spatial structure of a surface. The correlation length β^* is defined in turns of the Autocorrelation Function $\rho(\tau)$ by the relation $\rho(\beta^*) = 1/e$. For larger values of β^*, the surface were obtained by an additional procedure of lapping the abraded surfaces with 1 μm diamond paste for a short time. Asperity heights of each abraded surface were digitized by a Talysurf 4 with a fine tipped stylus. Each profile consisted of 100 digitized points at a sampling distance of 2 μm, thus giving a profile length of 0.2 mm, which is slightly greater than the nominal contact width for the conditions used in the contact analysis. Since the values of σ and β^* increase with the profile length, the surface roughness values σ and β^* obtained from the profile length, which is near to the nominal contact width, can be said to be representative for the contact analysis. For a given profile, the magnification of the surface height values is changed to obtain different values of vertical roughness while the spatial structure remains unchanged. In this way, a total of 110 different profiles were available for contact analysis.

In the contact analysis, the ball diameter is 12.7 mm, the material moduli of the upper and lower bodies $E_1 = E_2 = 207$ Gpa, Poisson's ratio $\nu = 0.3$, Hardness = 160 Hv for the specimen and the ball load is 10N giving a mean pressure 0.56 Gpa.

2.1 Effect of σ. Figure 1 shows the contact stresses and surfaces deformation at a mean pressure of $p_n = 0.56$ Gpa for three surfaces having decreasing σ but similar values of β^*. It can be seen from this set of Figures that for a constant β^*, as the roughness decreases, the area of contact increase and the state of changes from predominantly plastic to predominantly elastic and eventually reaches total conformity.

2.2 Effect of β^* Figure 2 shows the contact stresses and surface deformation at a mean pressure of $p_n = 0.56$ GPa for three surfaces having increasing β^* and similar σ values. Again there is tendency to three types of contact. As β^* increases, the contact changes from predominantly plastic to predominantly elastic. At large β^*, the contact tends to a state of total conformity.

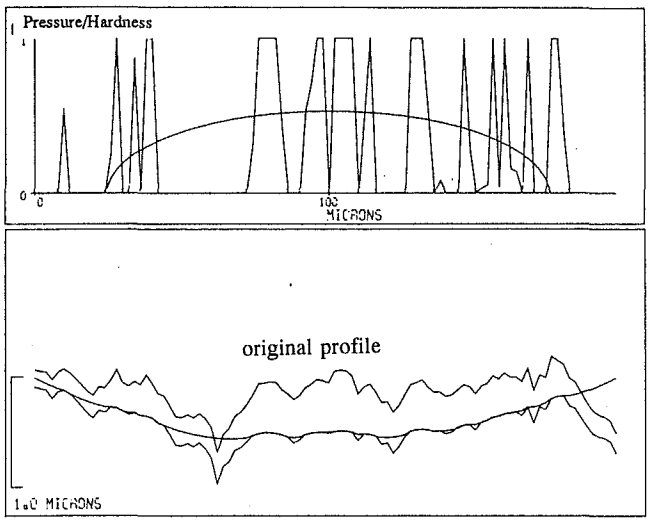

Fig. 1(*a*) Partial plastic contact

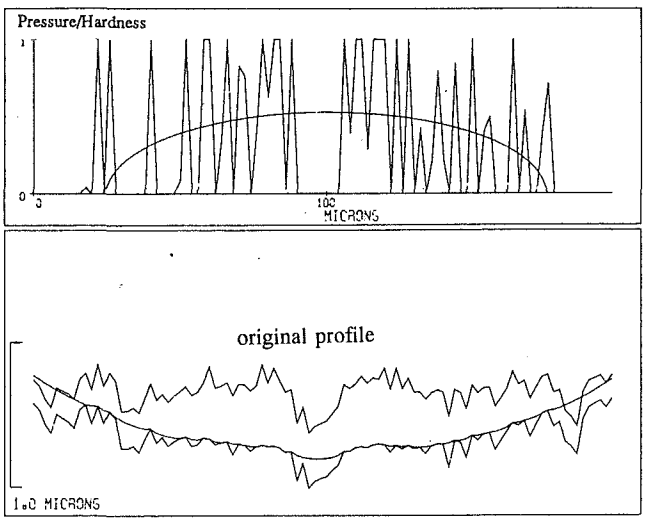

Fig. 2(*a*) Partial plastic contact

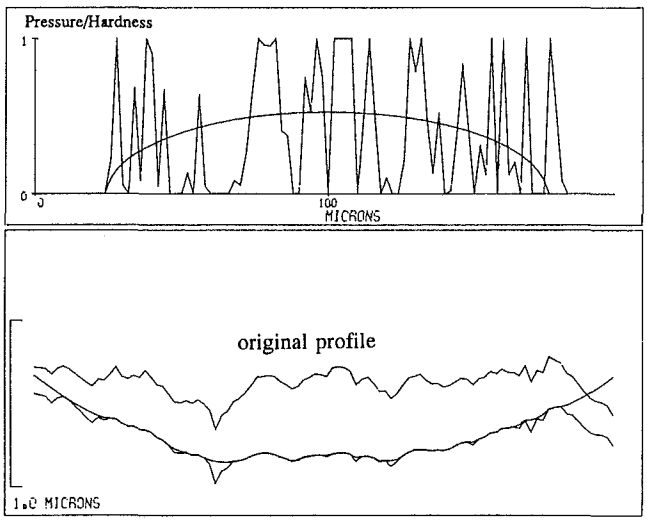

Fig. 1(*b*) Partial elastic contact

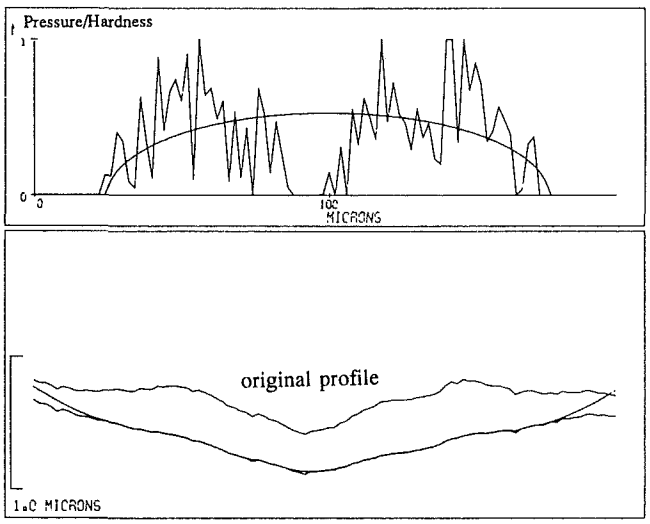

Fig. 2(*b*) Partial elastic contact

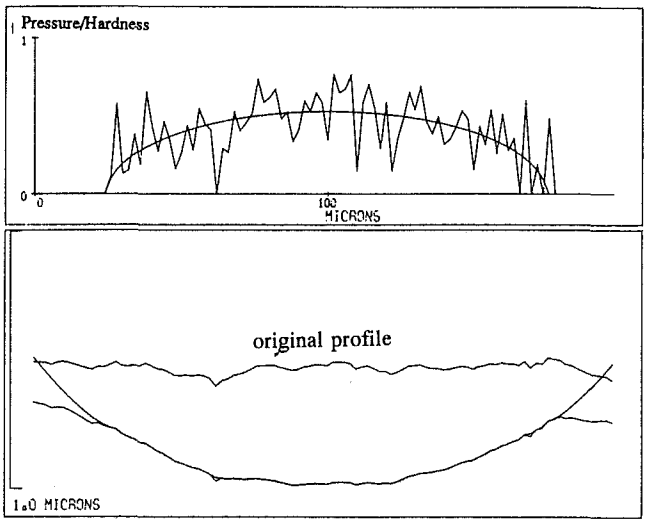

Fig. 1(*c*) Total elastic contact

Fig. 1 Three types of surface contact for three surfaces having decreasing σ but similar values of β^*. $p_n = 0.56$ Gpa, $H = 160$ H_v, $E_1 = E_2 = 207$ Gpa, $\nu_1 = \nu_2 = 0.3$

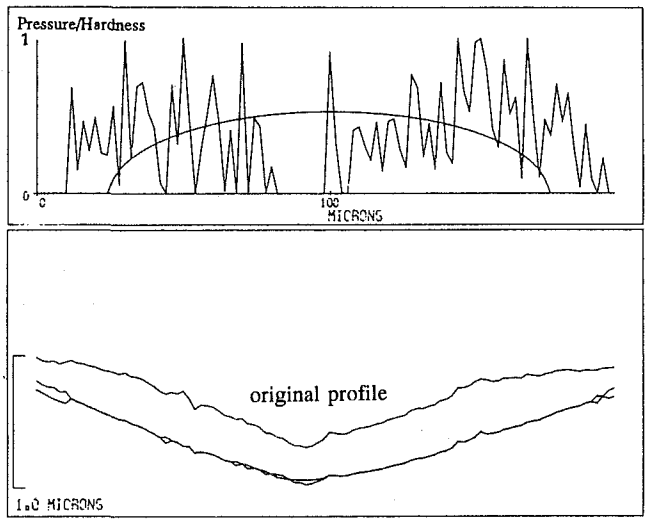

Fig. 2(*c*) Almost total elastic contact

Fig. 2 Three types of surface contact for three surfaces having increasing β^* but similar values of σ. $p_n = 0.56$ Gpa, $H = 160$ H_v, $E_1 = E_2 = 207$ Gpa, $\nu_1 = \nu_2 = 0.3$

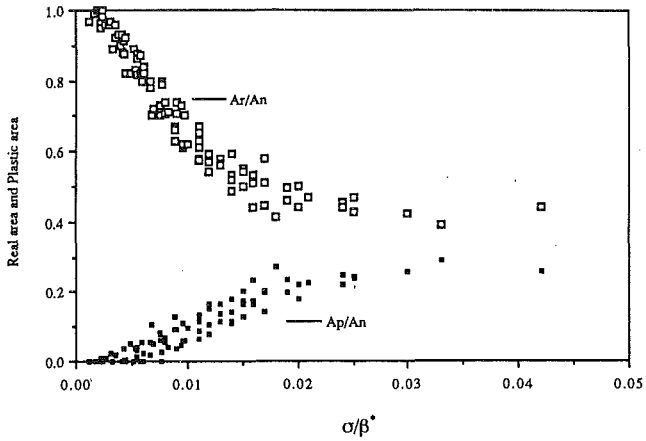

Fig. 3 Variation of real area and plastic area with σ/β^* for 110 surfaces with different combination of σ and β^*

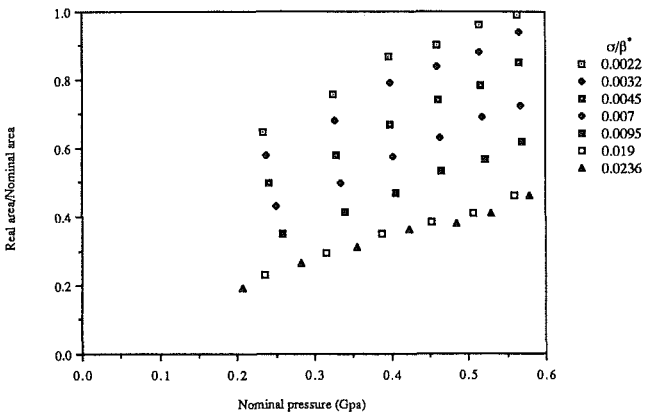

Fig. 4 Variation of real area with load for different σ/β^*

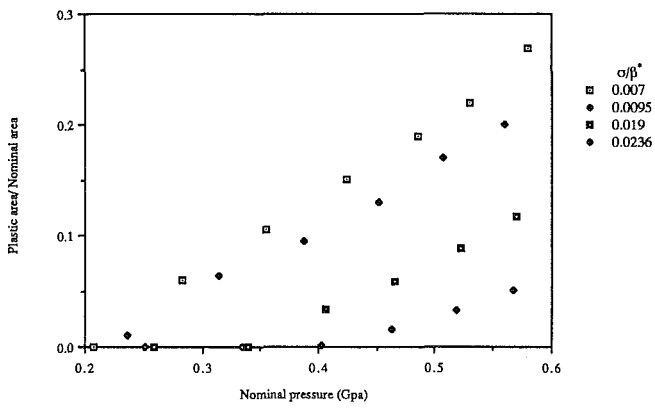

Fig. 5 Variation of plastic area with load for different σ/β^*

2.3 Effect of σ/β^* In the characterization of rough surfaces, it has been found that many surfaces contact conditions can be related to the ratio σ/β^* (Whitehouse and Archard, 1970). Indeed, the contact area can be related to σ/β^*, as shown in Fig. 3, which represents the results of 110 surface profiles with different σ and β^*.

At large σ/β^*, the asperity contact will be predominantly plastic. A value of the ratio of plastic area/real area A_p/A_r can be chosen to represent the mode of plastic deformation. At a very small σ/β^*, there exists a small but finite value of σ/β^* below which the real area is equal to the nominal area.

2.4 Effect of Load. It is generally believed that the real area is directly proportional to load for light loads. Here, the proportionality of the load-area relationship is investigated. Figures 4 and 5 show the variation of real area and plastic area with load for different σ/β^*. In all cases proportionality is seen to be valid over a limited range of pressure and this is usually the low pressure region. However, in some cases proportionality extends over a wide range of loads.

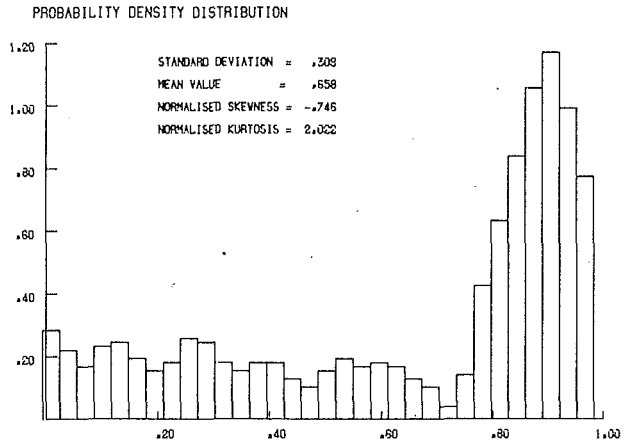

Fig. 6(*a*) $\sigma/\beta^* = 0.022$

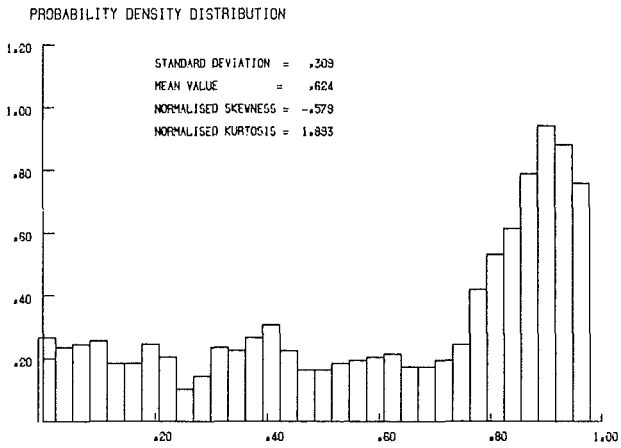

Fig. 6(*b*) $\sigma/\beta^* = 0.017$

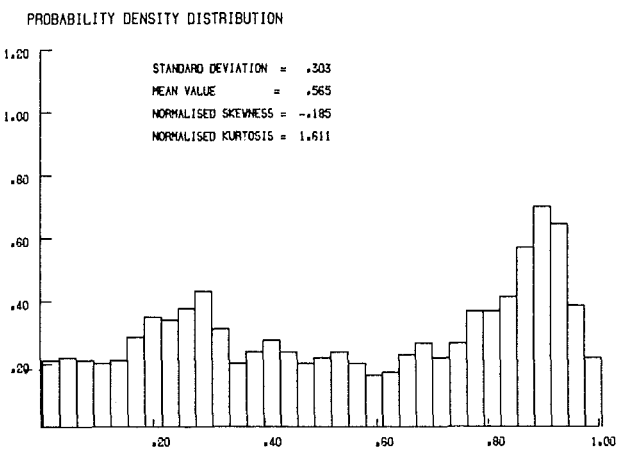

Fig. 6(*c*) $\sigma/\beta^* = 0.015$

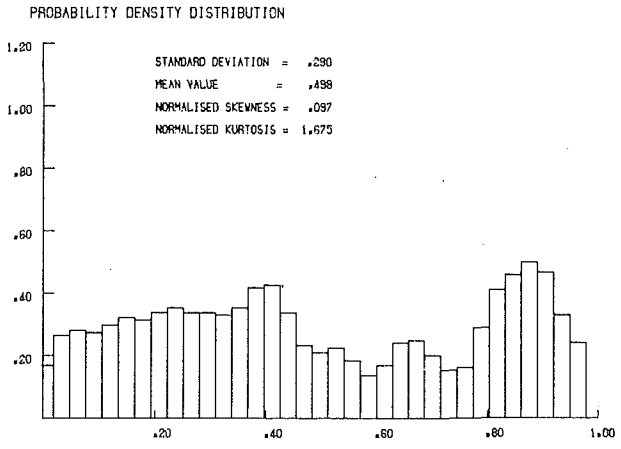

Fig. 6(*d*) $\sigma/\beta^* = 0.0126$

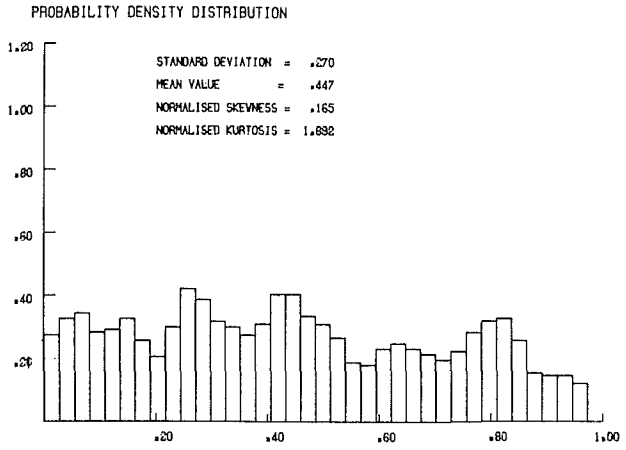

Fig. 6(*e*) $\sigma/\beta^* = 0.0064$

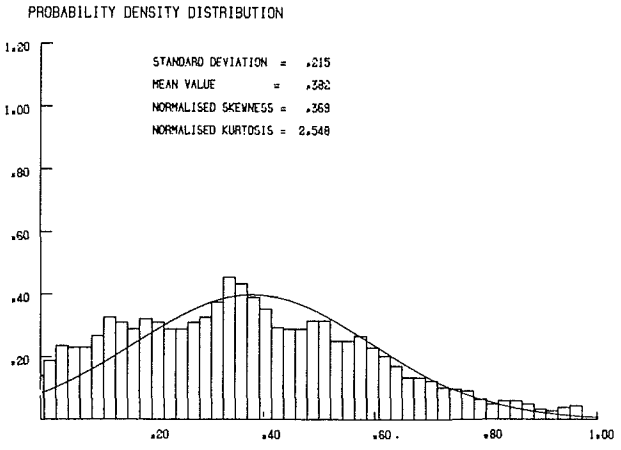

Fig. 6(*f*) $\sigma/\beta^* = 0.0047$

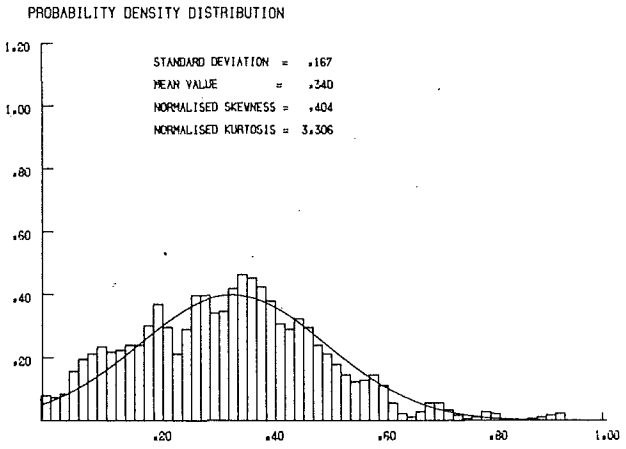

Fig. 6(*g*) $\sigma/\beta^* = 0.0028$

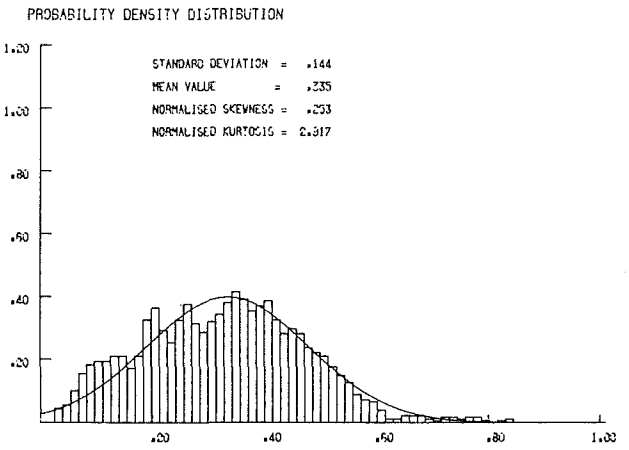

Fig. 6(*h*) $\sigma/\beta^* = 0.0013$

Fig. 6 Pressure distribution for different σ/β^*. $p_n = 0.56$ Gpa, $H = 160\ H_v$, $E_1 = E_2 = 207$ Gpa, $\nu_1 = \nu_2 = 0.3$.

2.5 Distribution of Contact Areas, Pressures, and Gaps. In this section, the distribution of contact areas, contact pressures and gaps for different σ/β^* are examined. In order to have enough sample data for the distribution curves to be representative, contact results obtained from 7 to 8 surfaces with the same ratio of σ/β at a mean pressure of $p_n = 0.56$ Gpa are used.

Figure 6 shows the distribution of contact pressure for different σ/β^*. The contact pressure is the average pressure in the y-direction. For large σ/β^*, the contact is predominantly plastic and for small σ/β^*, the contact is predominantly elastic. For $\sigma/\beta^* \leq 0.005$, the pressure distribution tends to a Gaussian form. For each distribution, the average pressure is calculated and the results are shown in Fig. 7. (The average pressure is the average value over the local contact asperity pressures and is not the nominal pressure.) The average pressure appears proportional to σ/β^*.

Figure 8 shows the distribution of contact areas for different σ/β^*. The log-normal distribution curve is superimposed for comparison. For large σ/β^*, the distribution is generally positively skewed. This means that the contact consists of a relatively large number of smaller contact spots. For an intermediate value of σ/β^*, for example, $0.006 < \sigma/\beta^* < 0.013$, the distribution is closely log-normal. As σ/β^* becomes smaller, the distribution tends to be negatively skewed. This indicates the contact is dominated by some larger contact spots. This can be interpreted as the individual contact spots merging together to form a larger spot as the surface becomes smoother.

Figure 9 shows the cumulative area distribution for different values of σ/β^*. The graph is scaled such that a straight line is produced when the distribution is log-normal. It can be seen that the distribution is closely log-normal for large σ/β^*. As

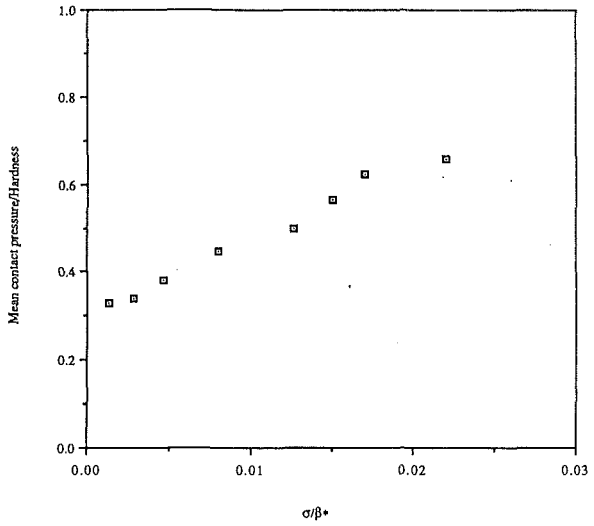

Fig. 7 Variation of mean contact pressure with σ/β^*. $p_n = 0.56$ Gpa, $H = 160\ H_v$, $E_1 = E_2 = 207$ Gpa, $v_1 = v_2 = 0.3$.

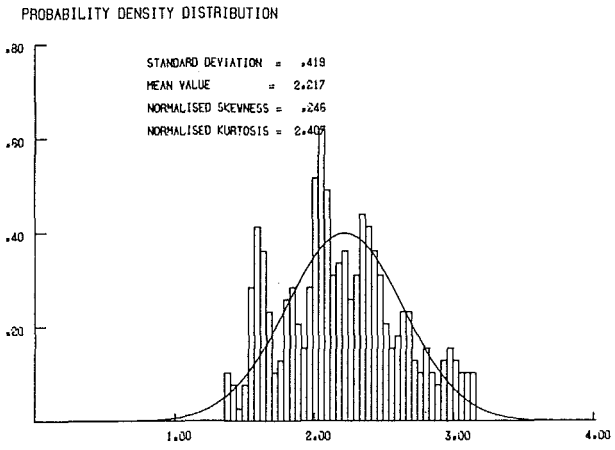

Fig. 8(*a*) $\sigma/\beta^* = 0.022$

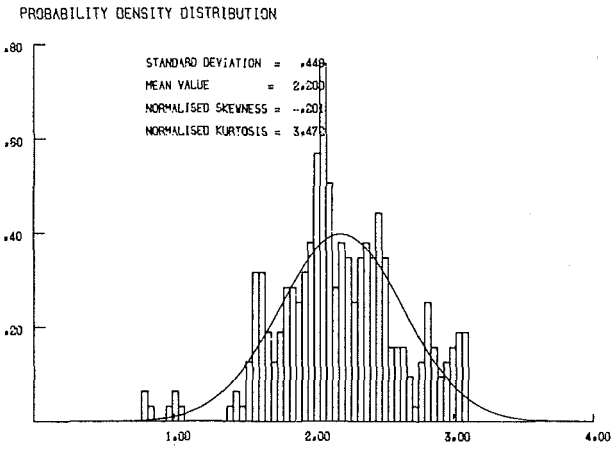

Fig. 8(*b*) $\sigma/\beta^* = 0.017$

σ/β^* becomes very small, the distribution does not follow a log-normal form. This may be due to the inadequacy of the area population as some smaller contacts merge together to form a larger contacts.

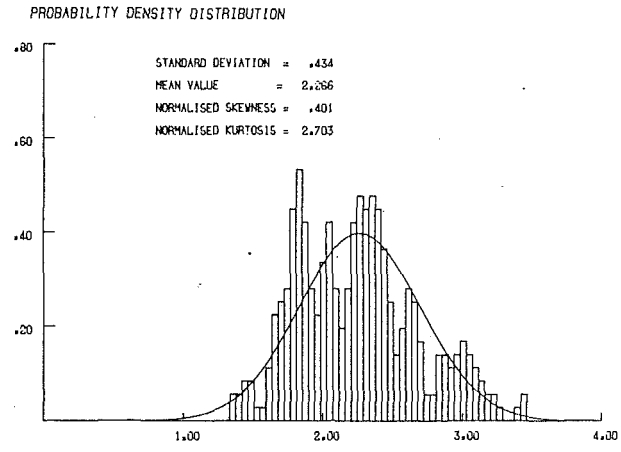

Fig. 8(*c*) $\sigma/\beta^* = 0.015$

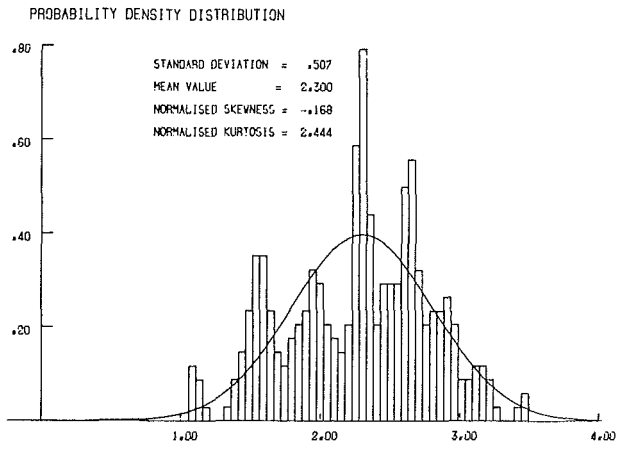

Fig. 8(*d*) $\sigma/\beta^* = 0.0126$

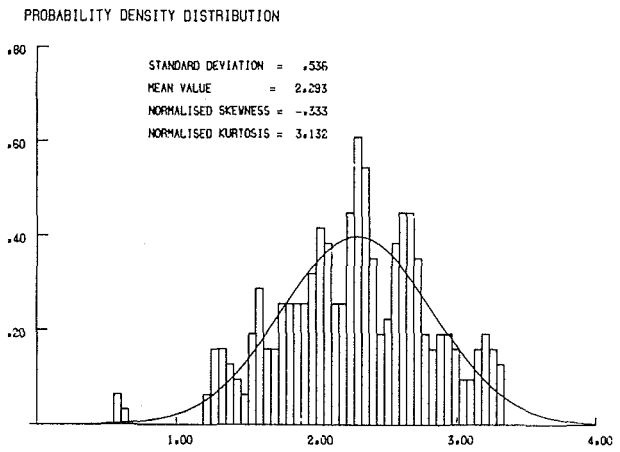

Fig. 8(*e*) $\sigma/\beta^* = 0.0064$

Figure 10 shows the contact area created by varying the height of the roughness of the same abraded surface under the same mean pressure of 0.56 Gpa. Some smaller contacts merge into a larger contact as the surface roughness decreases. Figure 11 shows the variation of the number of contact spots with σ/β^*. As expected, at small σ/β^*, the number of contact spots becomes smaller as a result of the merged contacts. As σ/β^*

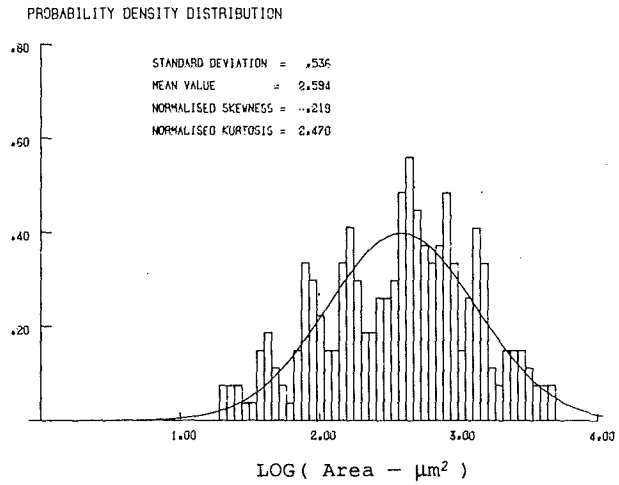

Fig. 8(*f*) $\sigma/\beta^* = 0.0047$

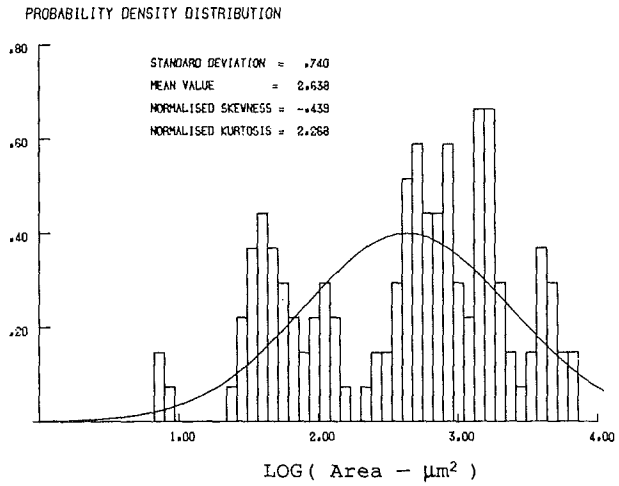

Fig. 8(*g*) $\sigma/\beta^* = 0.0028$

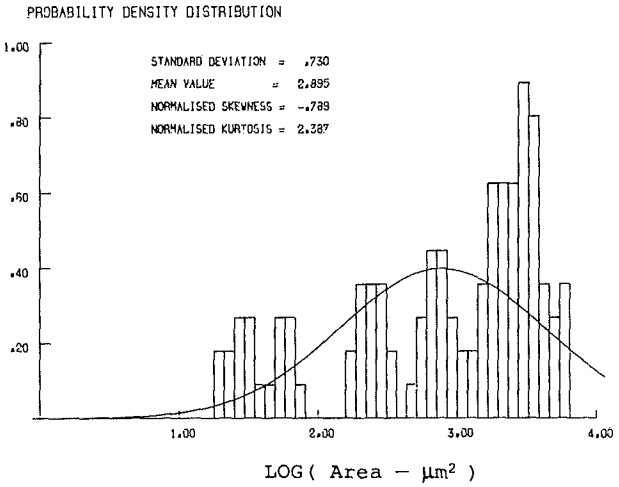

Fig. 8(*h*) $\sigma/\beta^* = 0.0013$

Fig. 8 Contact area distribution for different σ/β^*. $p_n = 0.56$ Gpa, $H = 160$ H_v, $E_1 = E_2 = 207$ Gpa, $v_1 = v_2 = 0.3$.

increases, the number of contact spots gradually increases until at large σ/β^*, it appears to approach a constant value.

The mean contact area for each distribution is calculated and shown in Fig. 12. The mean area changes very little over the range of σ/β^* used, but increases slightly for small σ/β^*.

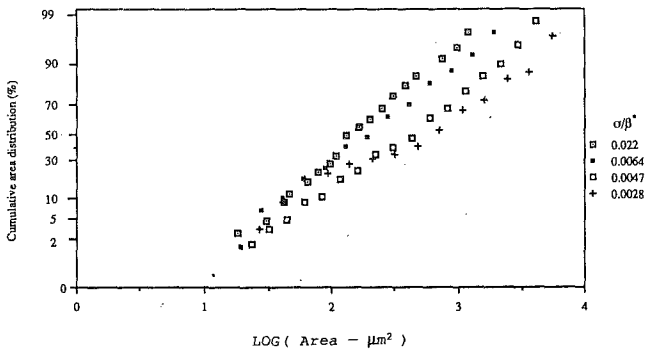

Fig. 9 Cumulative contact area distribution for various σ/β^*

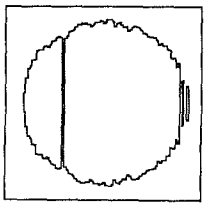

Fig. 10(*a*) $\sigma/\beta^* = 0.011$

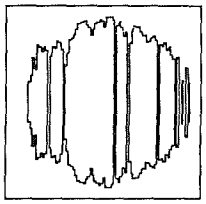

Fig. 10(*b*) $\sigma/\beta^* = 0.0032$

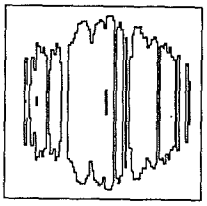

Fig. 10(*c*) $\sigma/\beta^* = 0.0045$

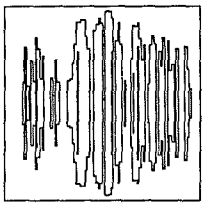

Fig. 10(*d*) $\sigma/\beta^* = 0.0095$

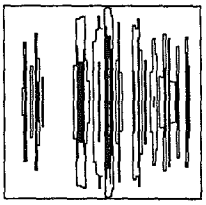

Fig. 10(*e*) $\sigma/\beta^* = 0.0147$

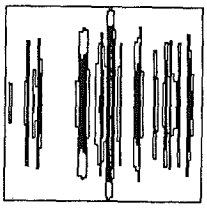

Fig. 10(*f*) $\sigma/\beta^* = 0.0236$

Fig. 10 Effect of increasing the surface roughness of a surface with the same β^* on the size of individual contact. $p_n = 0.56$ Gpa, $H = 160$ H_v, $E_1 = E_2 = 207$ Gpa, $v_1 = v_2 = 0.3$.

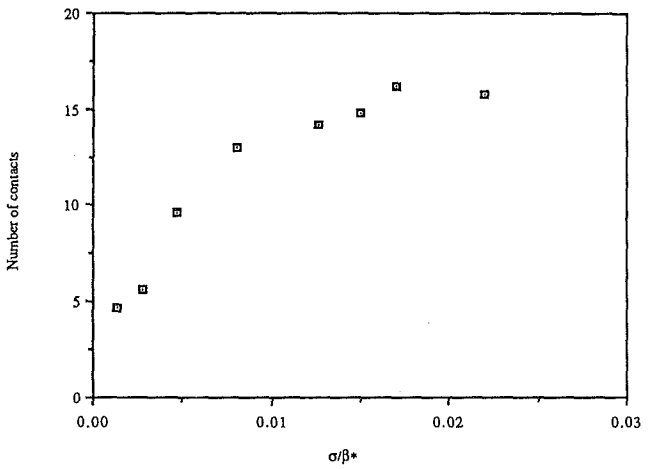

Fig. 11 Effect of σ/β^* on the number of individual contacts

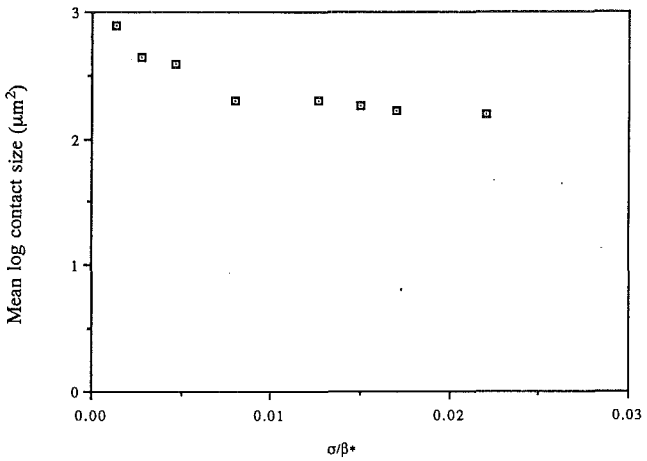

Fig. 12 Variation of mean contact area with σ/β^*

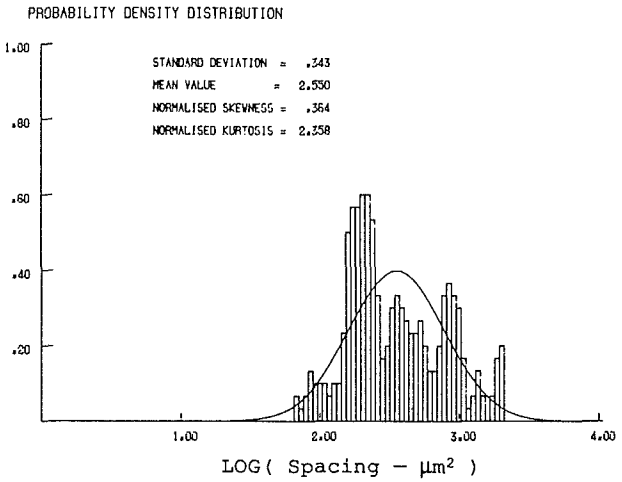

Fig. 13(*a*) $\sigma/\beta^* = 0.022$

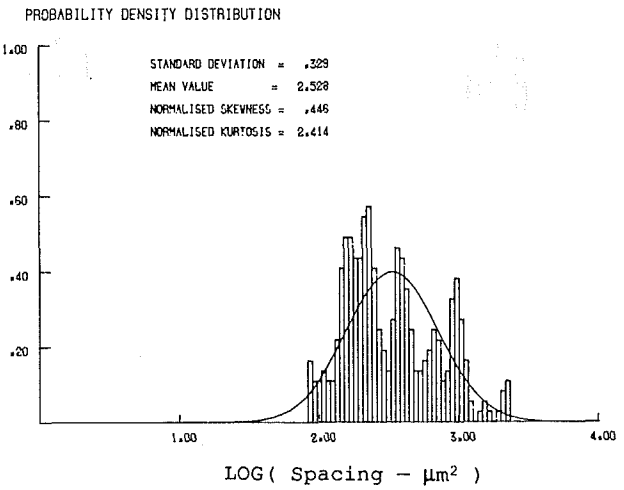

Fig. 13(*b*) $\sigma/\beta^* = 0.017$

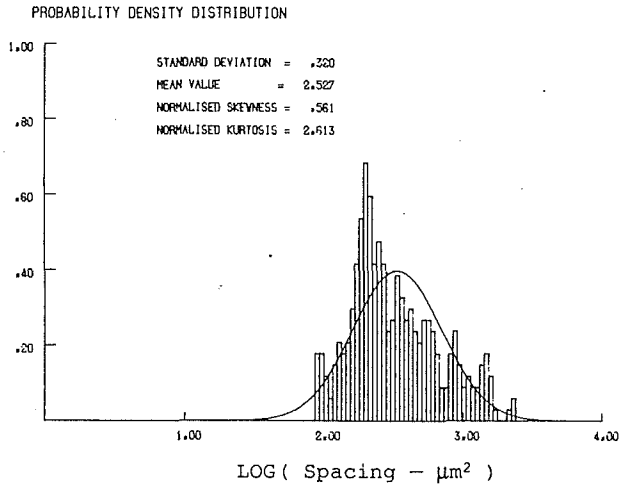

Fig. 13*c*) $\sigma/\beta^* = 0.015$

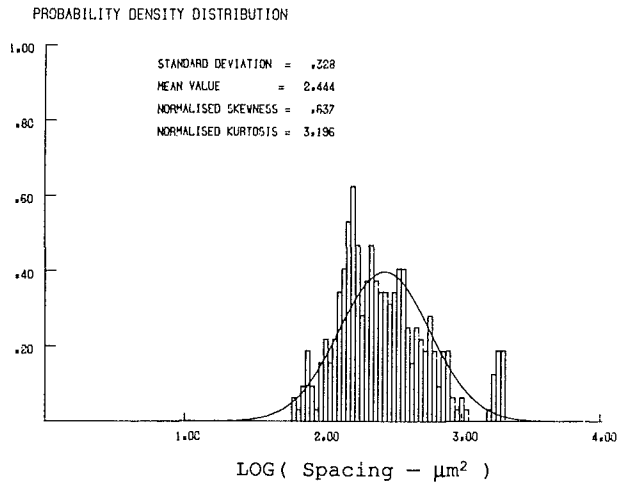

Fig. 13(*d*) $\sigma/\beta^* = 0.0126$

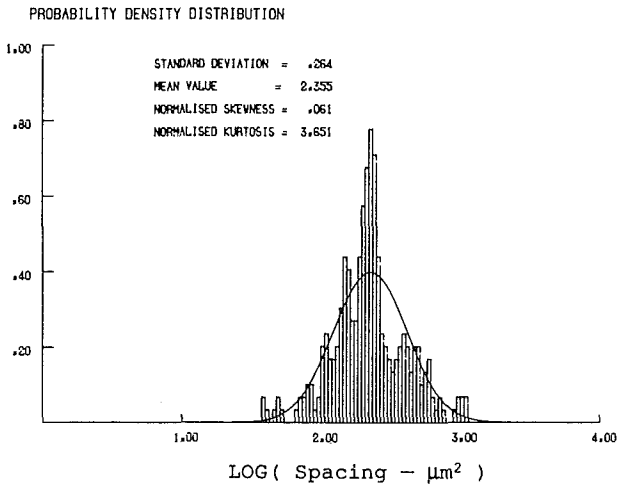

Fig. 13(*e*) $\sigma/\beta^* = 0.0064$

This result is in keeping with Greenwood's (1967) theory of how electrical contact resistance and friction theories can be explained in terms of a constant spot size.

Figure 13 shows the distribution of gaps for different σ/β^*. Unlike the distribution of contact area, the distributions are mostly positively skewed, indicating a larger population of smaller gaps between contacts.

Figure 14 shows the variation of the number of gaps with σ/β^*. At small σ/β^*, the number of gaps becomes smaller due to conformity. As σ/β^* increases, the number of gaps gradually increases until at large σ/β^*, it appears to approach a constant value.

For each distribution curve, the mean gap is calculated and shown as a function of σ/β^* in Fig. 15. The results show that the mean gap increases slightly with σ/β^*.

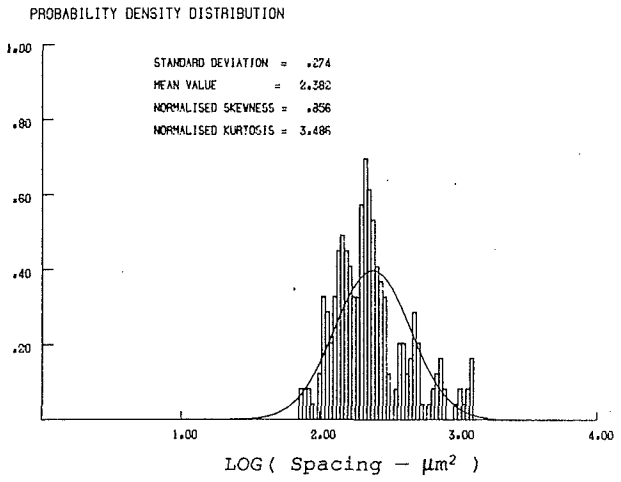

Fig. 13(*f*) $\sigma/\beta^* = 0.0047$

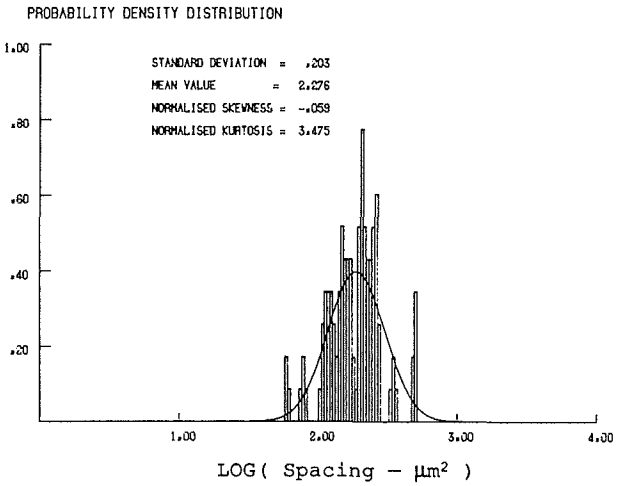

Fig. 13(*g*) $\sigma/\beta^* = 0.0028$

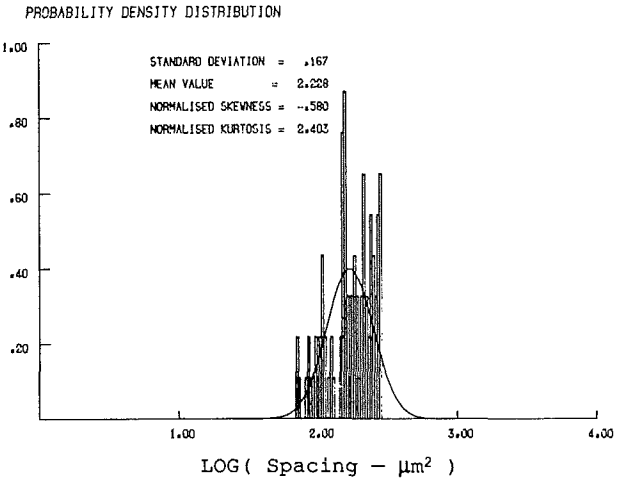

Fig. 13(*h*) $\sigma/\beta^* = 0.0013$

Fig. 13 Gap distribution for different σ/β^*. $p_n = 0.56$ Gpa, $H = 160$ H_v, $E_1 = E_2 = 207$ Gpa, $v_1 = v_2 = 0.3$.

2.6 Density of Contacts. The density of contacts D_c is defined as the number of contact elements divided by the total number of elements. Figure 16 (curve *a*) shows the variation of D_c with σ/β^*. The results show that the density of contacts decreases as σ/β^* increases. As σ/β^* becomes greater, the rate of decrease in D_c is smaller.

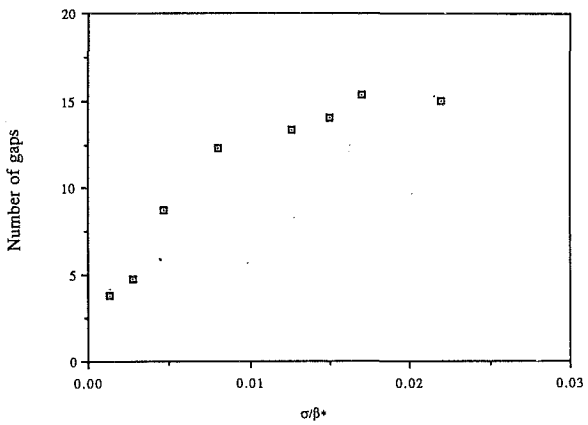

Fig. 14 Effect of σ/β^* on the number of gaps. $p_n = 0.56$ Gpa, $H = 160$ H_v, $E_1 = E_2 = 207$ Gpa, $v_1 = v_2 = 0.3$.

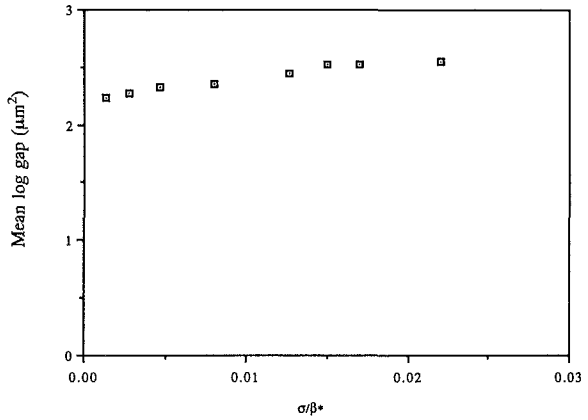

Fig. 15 Variation of mean gap with σ/β^*

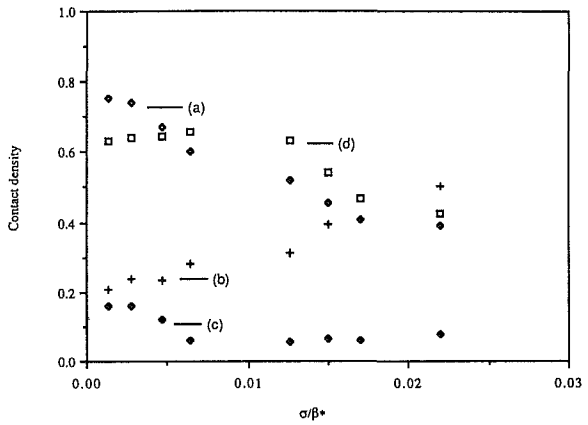

Fig. 16 Variation of contact density with σ/β^*: (*a*) number of contacts/number of elements; (*b*) number of peaks in contact/number of contacts; (*c*) number of valleys in contact/number of contacts; (*d*) number of shoulders in contact/number of contacts.

It is generally believed that contacts take place on the asperity tips and as a consequence wear and plastic deformation is confined to asperity peaks and the valleys remain untouched. For rough surfaces, the statement is reasonably acceptable. However, for very smooth surfaces, contacts can occur in the valleys due to significant amounts of elastic conformity. It is instructive to know among the contact how many are peak, valley or neither peak nor valley, as surface roughness varies. For convenience, a point which is neither a peak nor a valley

is called a shoulder. The proportion of contacts occurring on peaks, valleys and shoulders is also shown in Fig. 16 . The proportion of peaks among contacts increases with σ/β. At large σ/β^*, the contacts mainly occur on peaks, and the proportion of valleys in contacts varies only slightly. But as σ/β^* becomes smaller than 0.008, there is a definite increase in the proportion of valleys in contact. The proportion of contacts on shoulder does not change appreciably for $\sigma/\beta^* < 0.012$. But as $\sigma/\beta^* > 0.012$, it also decreases with σ/β^*.

3 Comparison of Numericl and Stochastic Results. Traditionally, load-area relationships have been derived by a stochastic approach. Bush et al. (1975) have studied the contact of strongly anisotropic rough surfaces and therefore provide a suitable model for comparison. Onions and Archard (1973) have provided a model for isotropic surfaces. Although exact agreement would not be expected, it is of interest to know how comparisons behave.

Bush et al. modeled the surface as parabolic ellipsoids having a Gaussian distribution of heights. They derived the following expressions for the relationship between the normal load W and the contact area A,

$$\frac{W}{A} = \frac{\Omega\pi(\bar{\lambda}^2 + \overline{k'^2})^{1/2}}{2^{3/2}\overline{k'}K(\bar{k})} \tag{1}$$

where

$$\overline{k'} = \frac{0.4777\bar{\lambda}}{1 - 1.3211\bar{\lambda}} \tag{2}$$

$$\Omega = \sqrt{\frac{m_{02}}{\pi}}\, E' \tag{3}$$

$$\bar{\lambda} = \left(\frac{m_{20}}{m_{02}}\right)^{1/2} \tag{4}$$

$$\bar{k} = (1 - \overline{k'^2})^{1/2} \tag{5}$$

$$E' = \left[\frac{1-\nu_1^2}{E_1} + \frac{1-\nu_2^2}{E_2}\right]^{-1} \tag{6}$$

m_{02} and m_{20} are spectral moments in orthogonal directions, λ is the anisotropic bandwidth parameter and $K(k)$ is the complete elliptical integral of the first kind.

In order to apply the Bush model to compare with the numerical model, the value of λ is chosen 0.01, which corresponds to a very high degree of anisotropy. The elliptical integral is evaluated using tables (Dwight, 1966) for $\lambda = 0.01$, thus the theory of Bush can be stated as $W/A = 0.214E'\sqrt{m_2}$.

Onions and Archard modeled the surface as possessing a Gaussian height distribution with an exponential autocorrelation function, and derived an expression for isotropic surfaces, i.e., $W/A = 0.3'\sigma/\beta^*$.

The numerical results are summarized in Table 1. Figure 17 shows the load/contact area results from the numerical contact model plotted against $E'\sqrt{m_2}$. West et al. (1987), using numerical analysis of a two-dimensional contact of a cylinder on a nominally rough surface, have shown that their results agree well with Bush's theory. Their results are also shown for comparison in Fig. 17. The straight line gives the result from Bush's analysis. The agreement is good for surfaces with $E'\sqrt{m_2} > 0.002$. However, for surfaces with small $E'\sqrt{m_2}$, the results appear to deviate. The deviation can be explained by conformity and the effect of concentrated contacts. For very smooth surfaces, it has been shown that the contact area approaches the nominal area which is given by,

$$A_n = \pi\left(\frac{3WR}{4E'}\right)^{2/3} \tag{7}$$

Table 1 Numerical results for load/area analysis

Surfaces	σ (μm)	β^* (μm)	m_2	W/A (N/μm^2)
1	0.005	4.60	4.55E-6	4.85E-4
2	0.079	4.73	1.43E-4	7.09E-4
3	0.065	7.80	3.03E-4	7.36E-4
4	0.041	18.4	2.96E-5	5.00E-4
5	0.156	17.8	1.86E-4	8.00E-4
6	0.114	26.8	1.97E-4	5.66E-4
7	0.015	3.40	3.64E-5	5.83E-4
8	0.190	6.25	3.67E-3	13.5E-4
9	0.180	7.54	2.51E-3	11.9E-4
10	0.046	5.80	1.51E-4	7.54E-4
11	0.065	6.20	2.74E-4	8.30E-4
12	0.068	6.12	2.82E-4	7.71E-4
13	0.046	4.72	3.01E-4	7.56E-4

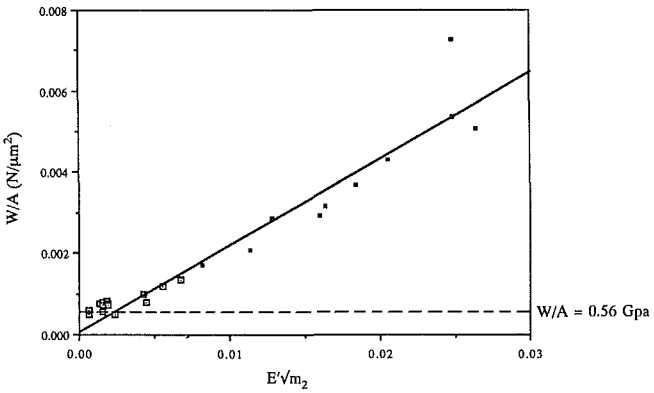

Fig. 17 Variation of load/area results with $E'\sqrt{m_2}$. □ Rough surface contact results; ■ West and Webster results; — from Bush's theory.

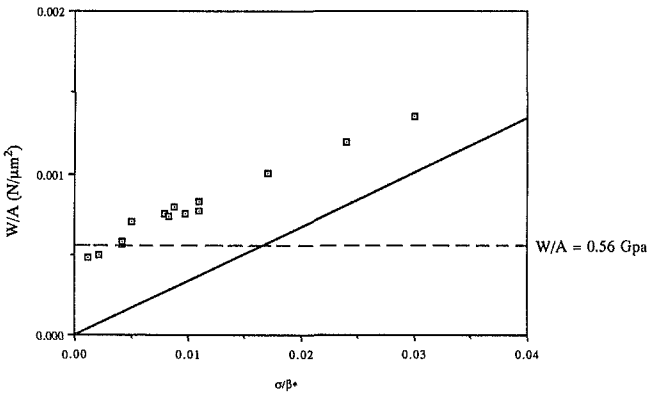

Fig. 18 Variation of load/area of σ/β^*. The straight line gives the results from Onions and Archard's theory.

where W is the load and R is the radius of the ball. Then the load/area is given by,

$$\frac{W}{A_n} = \frac{4E'W^{1/3}}{3\pi R} \tag{8}$$

Therefore, for a conforming surface W/A is proportional to $W^{1/3}$ and inversely proportional to the radius R. Thus the results for a ball with a small radius are expected to be higher than results for two nominally flat contacts.

The average W/A_n is given by the nominal pressure which is 0.56 Gpa. Therefore, the load/area results would be expected to converge to 0.56 Gpa as shown in Fig. 18 when the surfaces become very smooth. As the surface roughness increases, the contacts are fewer and the load is spread more evenly like that shown in Figs. 1 and 2. In this case the effects of having so called concentrated contacts become less significant and results agree equally well with Bush's theory for nominally flat sur-

faces, and with the results of West and Webster for 2-D cylindrical contacts.

Figure 18 shows the W/A results from the numerical model plotted against σ/β^*. The straight line gives the results from Onions and Archard's theory. Exact agreement would not be expected because in Onions and Archard's model the surface roughness was assumed to be isotropic. From the figure, as σ/β^* becomes smaller, the load/area value approaches the value given by the nominal pressure.

4 Conclusions

A numerical elastic-plastic contact model has been used to analyze a sample set of rough surface profiles. The real area and plastic area are found to dependent on the ratio σ/β^*. For a particular value of σ/β^*, the real and plastic area can be determined by the curve shown in Fig. 3. In general, there exists different types of contact depending on the value of σ/β^*. For large σ/β^*, the contact is predominantly plastic. The area is less dependent on σ/β^*. For intermediate σ/β^*, the contact is predominantly elastic. As σ/β^* becomes smaller, there exists a finite value of σ/β^* such that the real area is equal to the nominal area.

The load-area relationship for different σ/β^* has been investigated. The hypothesis that the real area of contact is proportional to load has been shown to be approximately true for surfaces with the intermediate values of σ/β^* and large values of σ/β^* at relatively low loads. For a surface with a very small value of σ/β^*, the real area approaches the nominal area asymptotically. Results have been compared with Bush's stochastic contact model for highly anisotropic rough surfaces and agreement is good for surfaces with relatively large values of σ/β^*. However, as σ/β^* becomes smaller, the load/area approaches the values given by the nominal pressure for smooth surface contacts.

The distribution of contact pressures, contact areas, and gaps have been investigated for various σ/β^*. The distribution of pressures can follow a Gaussina form for intermediate σ/β^* or small σ/β^* while the distributions become skewed towards the flow pressure of the softer material at large σ/β^*.

In general, the distribution of contact areas follows a Gaussian form for intermediate and high values of σ/β^*. The average size and number of the contact spots does not vary appreciably for intermediate and large values of σ/β^*. But at small values of σ/β^*, the number of contact spots is small and their sizes are large.

The distribution of gaps is generally positively skewed for all values of σ/β^*. The average gap increases slightly with σ/β^*. For small σ/β^* the number of gaps is small. The number of gaps increases with σ/β^* and approaches a contact at value at large σ/β^*.

References

Bush, A. W., Gibson, R. D., and Thomas, T. R., 1975, "The Elastic Contact of a Rough Surfaces," *Wear*, Vol. 35, pp. 87–111.

Bush, A. W., Gibson, R. D., and Keogh, G. P., 1979, "Strongly Anisotropic Rough Surfaces," ASME JOURNAL OF LUBRICATION TECHNOLOGY, Jan., Vol. 101, pp. 15–20.

Dwight, H. B., 1966, Tables of Integrals and Other Mathematical Data, 4th ed., Macmillan, New York, NY.

Greenwood, J.A., 1967, "The Area of Contact Between Rough Surface and Flat," *Trans.*, ASME, Vol. 89, pp. 81–91.

Greenwood, J. A., and Williamson, J. B. P., 1966, "Contact of Nominally Flat Surfaces," *Proc. Soc. Lond.*, A295, pp. 300–319.

Nayak, P. R., 1971, "Random Process Model of Rough Surfaces," ASME JOURNAL OF TECHNOLOGY, Vol. 93, pp. 398–407.

Onions, R. A., and Archard, J. F., 1973, "The Contact of Surfaces Having a Random Structures," *J. Phy. D: Applied Phys.*, Vol. 6, pp. 289–304.

Poon, C. Y., and Sayles, R. S., 1993, "Numerical Contact Model of a Smooth Ball on an Anisotropic Rough Surface," ASME JOURNAL OF TRIBOLOGY, Vol. 116, pp. 194–201.

Sayles, R. S., and Thomas, T. R., 1978, "Computer Simulation of the Contact of Rough Surfaces," *Wear*, Vol. 49, pp. 273–296.

Webster, M. N., and Sayles, R. S., 1986, "A Numerical Model for the Elastic Frictionless Contact of Real Rough Surfaces," ASME JOURNAL OF TRIBOLOGY, Vol. 108, pp. 314–320.

West, M. A., Webster, M. N., and Sayles, R. S., 1987, "A New Method for Rough Surface Contact Analysis," *Proc. Inst. Mech. Engrs., Tribology-Friction, Lubrication and Wear Fifty Years*, pp. 945–955.